

**Transient genomic instability drives tumorigenesis
through accelerated clonal evolution**

Ofer Shoshani¹, Bjorn Bakker², Lauren de Haan^{1,2}, Andréa E Tjihuis², Yin Wang¹, Dong Hyun Kim¹, Marcus Maldonado¹, Matthew A. Demarest¹, Jon Artates¹, Ouyang Zhengyu³, Adam Mark⁴, Rene Wardenaar², Roman Sasik⁴, Diana C.J. Spierings², Benjamin Vitre^{1,5}, Kathleen Fisch⁴, Floris Foijer^{2,6}, and Don W. Cleveland^{1,6}

¹ Ludwig Cancer Research and Department of Cellular and Molecular Medicine, University of California at San Diego, La Jolla, CA, USA.

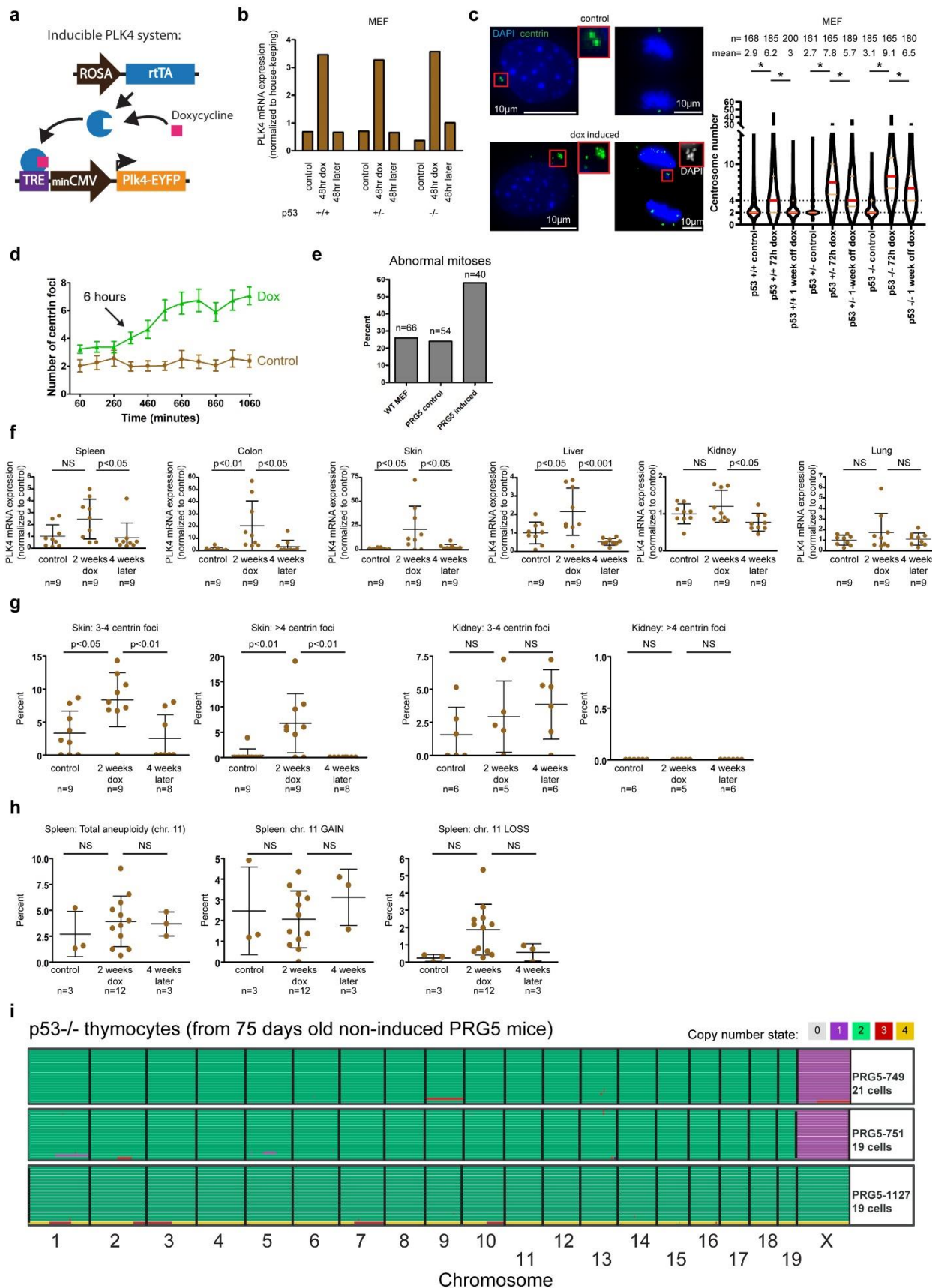
² European Research Institute for the Biology of Ageing (ERIBA), University of Groningen, University Medical Center Groningen, 9713 AV, Groningen, The Netherlands.

³ Department of Cellular and Molecular Medicine, University of California at San Diego, La Jolla, CA, USA.

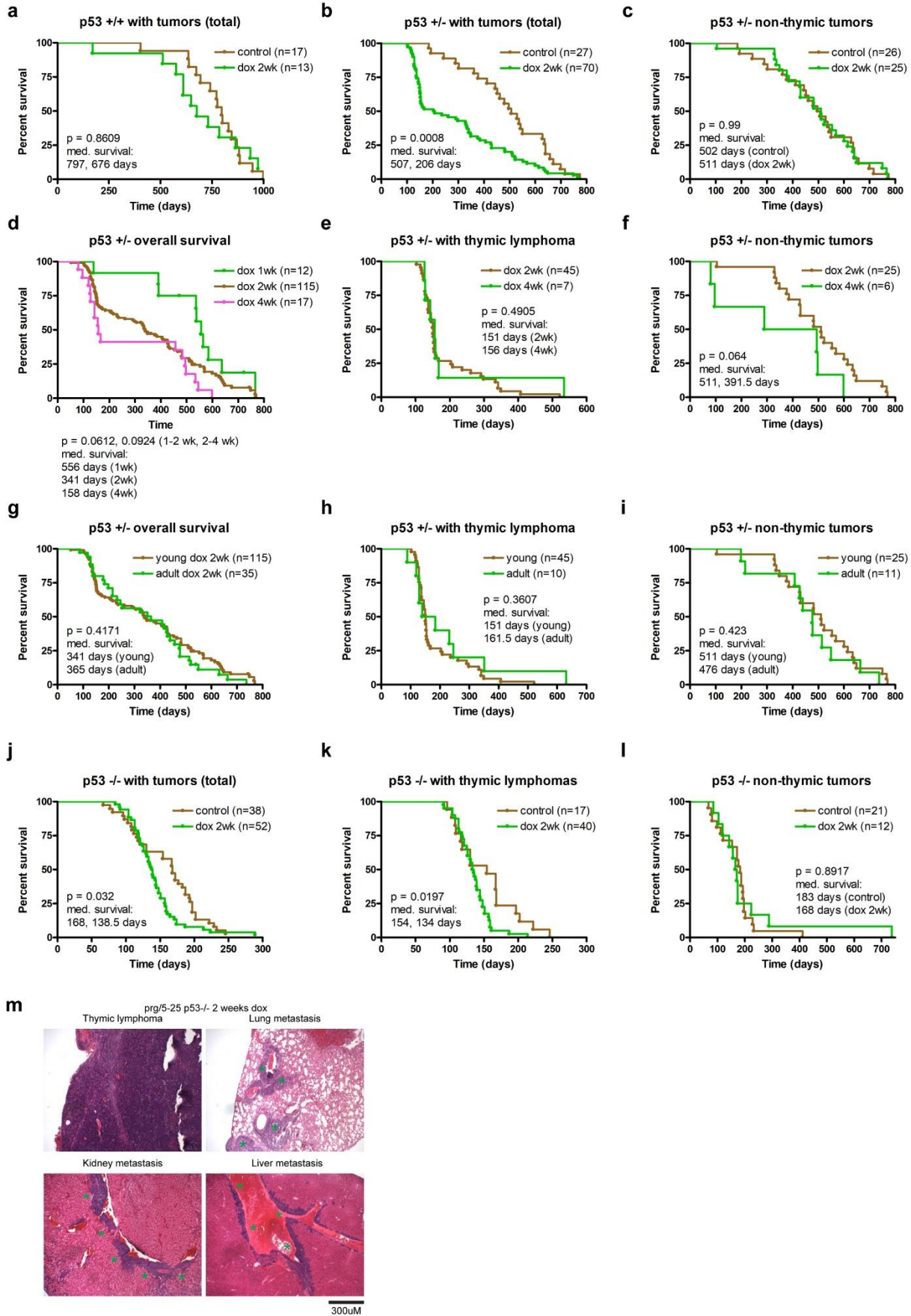
⁴ Center for Computational Biology & Bioinformatics, Department of Medicine, University of California, San Diego, La Jolla, CA, USA.

⁵ Current affiliation: CRBM, Univ Montpellier, CNRS, Montpellier, France.

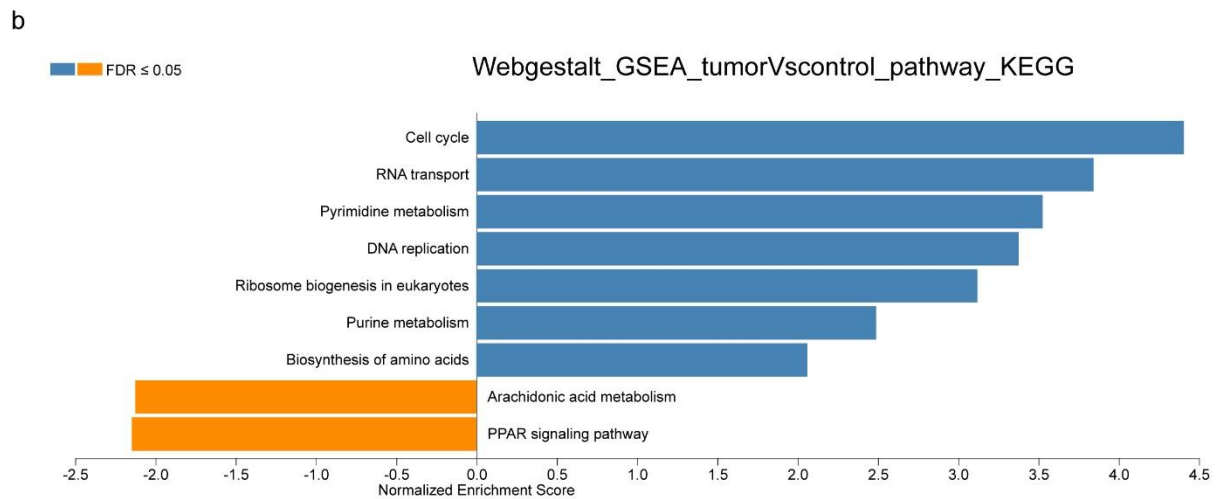
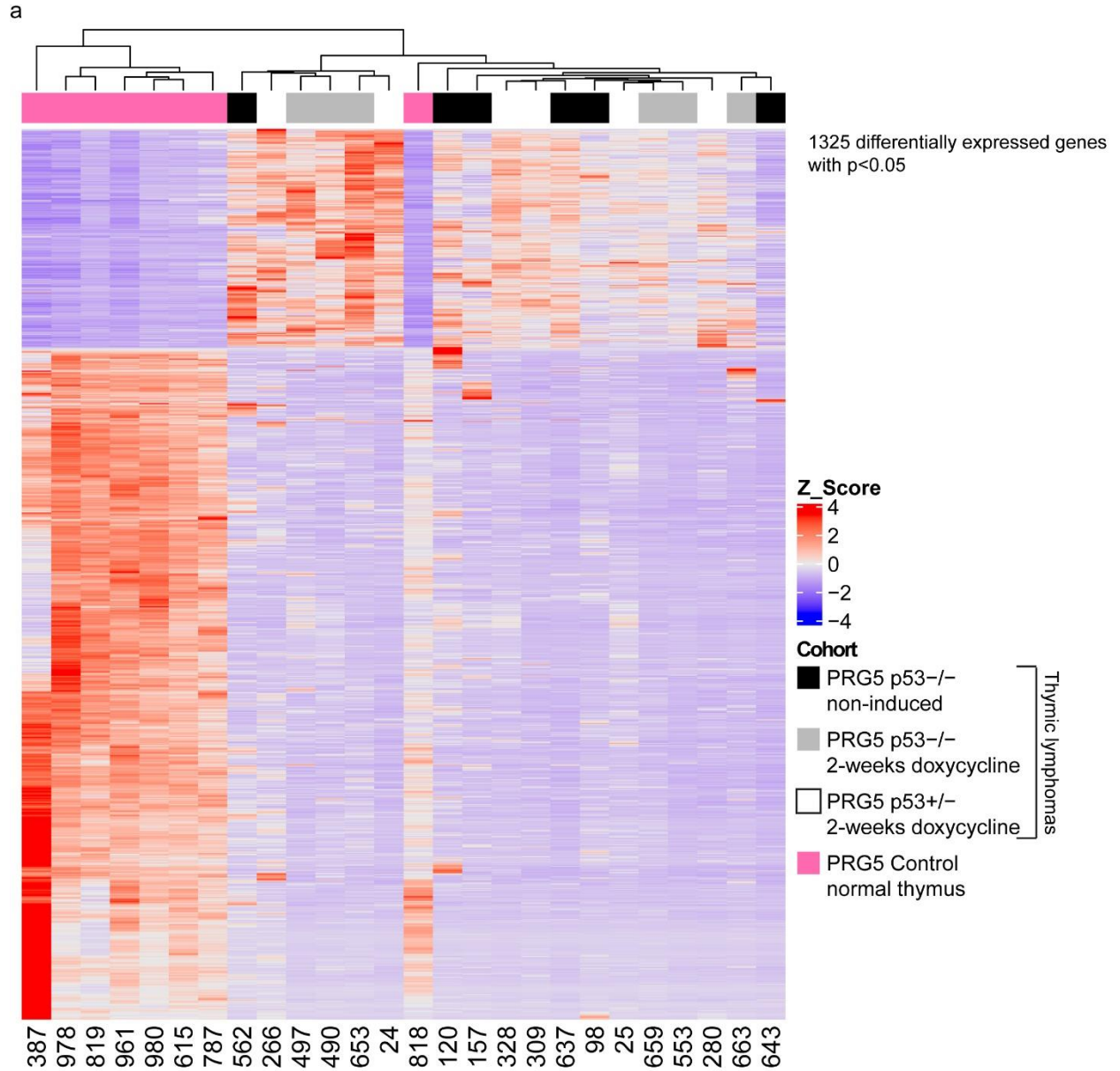
⁶ Corresponding authors: dcleland@health.ucsd.edu (D.W.C.), f.foijer@umcg.nl (F.F.)



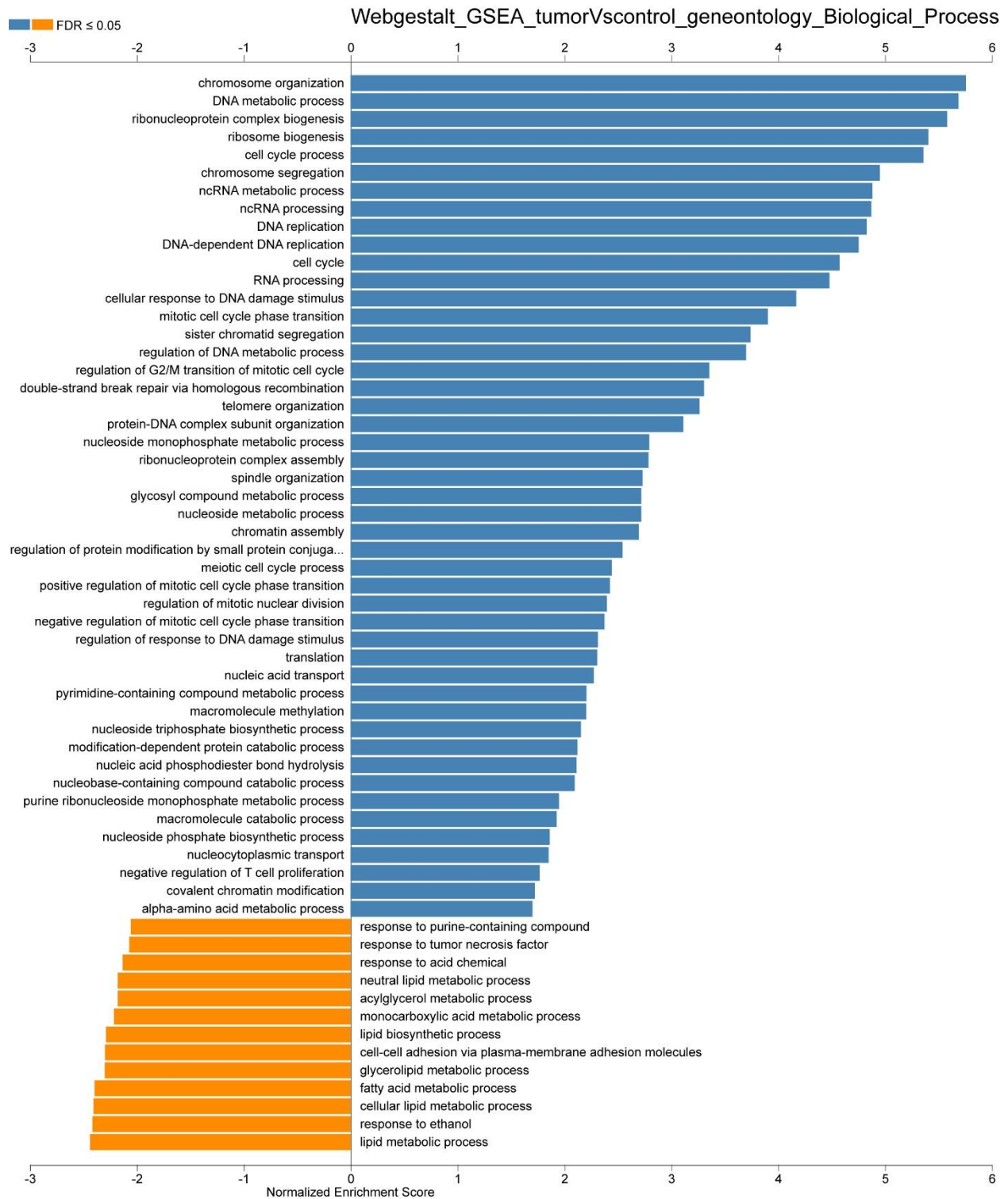
Supplemental Figure S1 | Effect of PLK4 overexpression in vitro and in vivo. (a) Inducible Plk4 expression using the tetracycline-on system. Doxycycline provided in mouse chow binds the reverse tetracycline-controlled trans-activator (rtTA, inserted in the Rosa locus) that together bind a Tet Response Element (TRE) upstream of Plk4 (inserted into the Col1A locus). **(b)** Plk4 mRNA levels in mouse embryonic fibroblasts derived from p53^{+/+}, p53^{+/-}, and p53^{-/-} PRG5 mice, before (control) immediately after (48hr dox) and 48 hours after (48hr later) doxycycline administration. **(c)** Frequency of centrosome amplification as determined using centrin-GFP in mouse embryonic fibroblasts derived from p53^{+/+}, p53^{+/-}, and p53^{-/-} PRG5 mice, before (control) immediately after (72hr dox) and 1 week after (1 week off dox) doxycycline administration. Violin plots show median (red) and quartiles (orange). *p<0.0001 determined using one-way ANOVA with Tukey's Multiple Comparison Test. Data from two independent experiments are presented. Representative images of control and doxycycline induced MEFs are shown. **(d)** Measurements of centrin-GFP foci (starting one hour following Plk4 induction, mean \pm SD, n=37-54 and n=43-77 per time point for control and induced cells, respectively). **(e)** Mitotic abnormalities (anaphase bridges and lagging chromosomes) in p53^{+/-} control PRG5 MEFs, or starting 8 hours after Plk4 induction, and in wild-type MEFs (C57BL/6 mice). Similar levels of basal CIN were observed in both wild-type MEFs and in control PRG5 MEFs indicating there is minimal or no leakiness in the Plk4 doxycycline system. **(f-h)** Plk4 mRNA levels **(f)**, measurement of centrin-GFP foci **(g)**, and percent aneuploidy for chromosome 11 (using interphase DNA-FISH, **h**) in induced tissues from PRG5 mice before (control) immediately after (2 weeks dox) and one month after (4 weeks later) doxycycline administration. Mean \pm SD of indicated mice per group are presented. *p-values determined using one-way ANOVA with Tukey's Multiple Comparison Test. **(i)** Heatmaps showing DNA copy number using single cell whole-genome sequencing of cells collected from normal thymic tissues of 75-days old p53^{-/-} PRG5 mice.



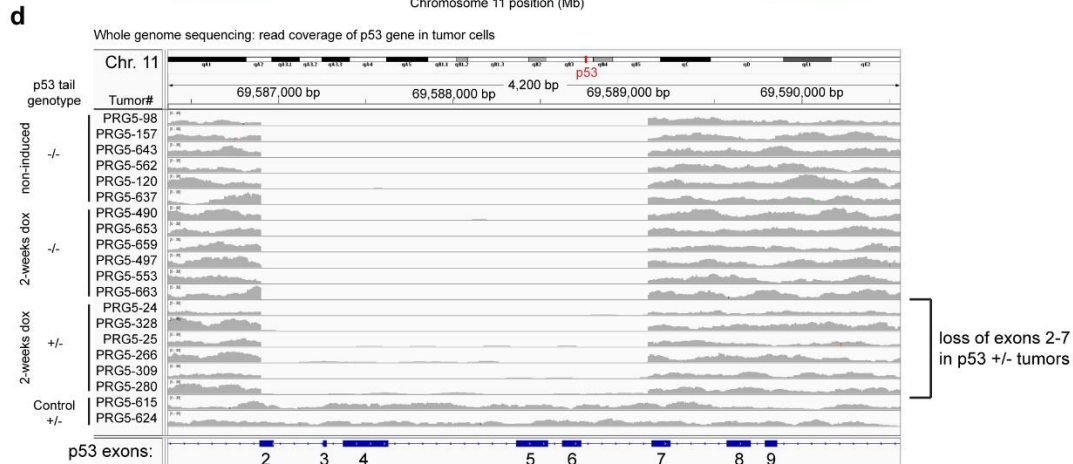
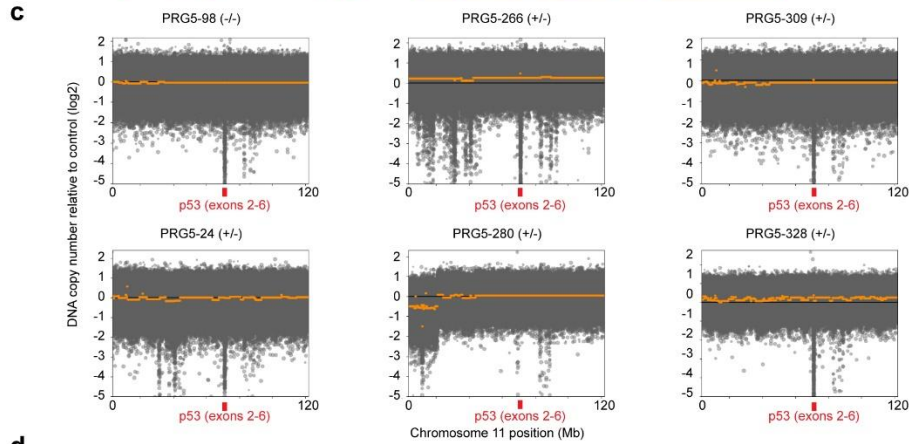
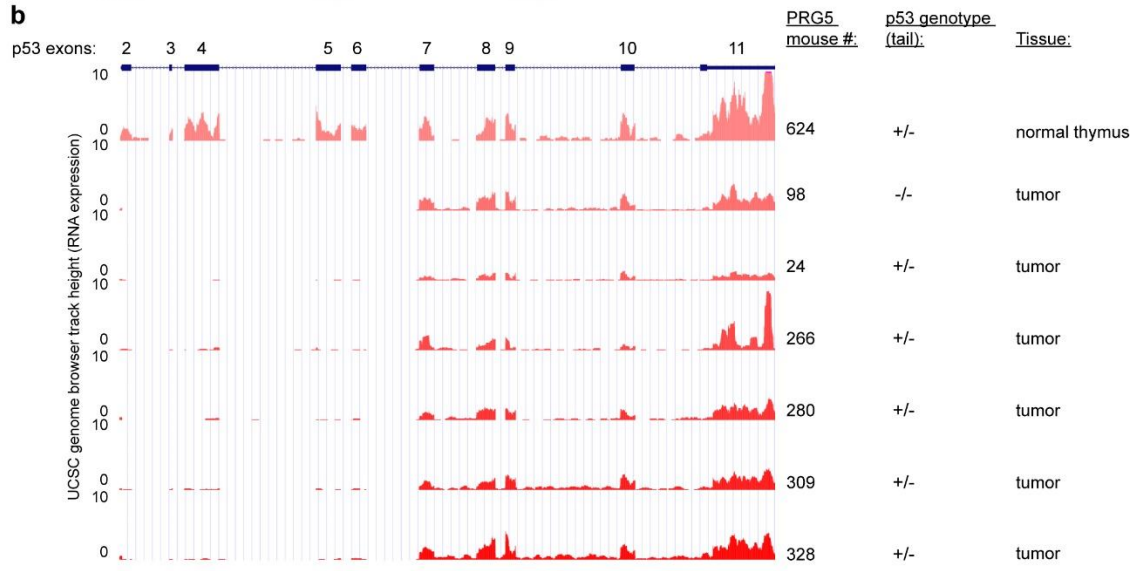
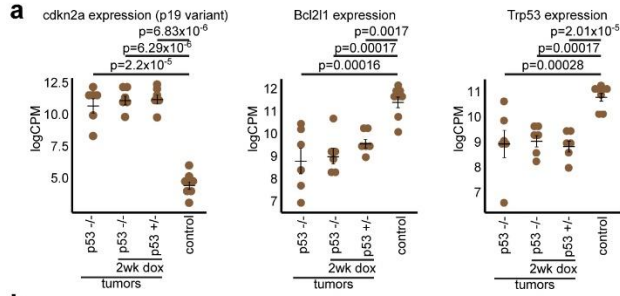
Supplemental Figure S2 | Effects of timing and duration of chromosome instability on tumor formation. (a-l) Survival (Kaplan-Meier) plots of PRG5 mice not treated (control) or treated with the indicated doxycycline regimens (dox 1wk/2wk/4wk – treated with doxycycline for 1/2/4 weeks at the age of 30 days; young/adult dox 2wk – 2 weeks treatment of doxycycline starting at 30/100 days of age) and with the indicated p53 backgrounds (p53^{+/+}, p53^{+/-}, p53^{-/-}). Overall survival and survival of mice bearing either thymic or non-thymic tumors are presented. Comparison of indicated number of mice done using log rank test. (m) Representative images of thymic lymphoma metastases from a 2-weeks Plk4 induced p53^{-/-} PRG5 mouse. See Supplemental Table 1 for a histology analysis of tissues from a total of 104 mice.



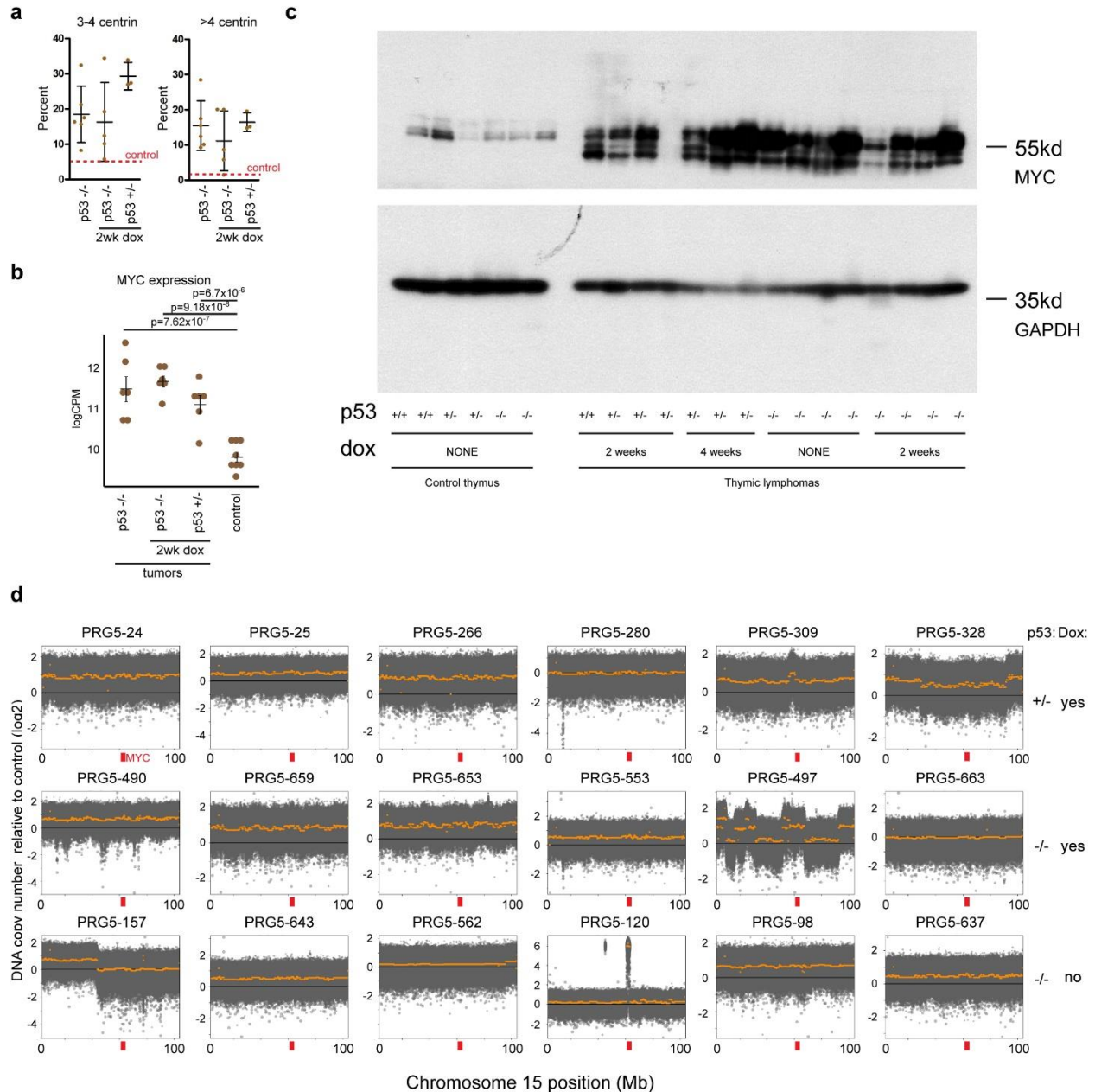
Supplemental Figure S3 | Differential gene expression analysis comparing thymic lymphomas and normal thymus. (a) Differentially expressed genes as determined using RNA sequencing between control normal thymuses and PRG5 derived thymic lymphomas. See Supplemental Table 2 for a complete list of the differentially expressed genes (b) Significantly enriched KEGG pathways in control thymuses and in PRG5 derived thymic lymphomas determined using Webgestalt GSEA analysis.



Supplemental Figure S4 | Pathway analysis reveals differences between thymic lymphomas and normal thymus. Significantly enriched Gene Ontology (Biological Processes) pathways in control thymuses and in PRG5 derived thymic lymphomas determined using Webgestalt GSEA analysis.

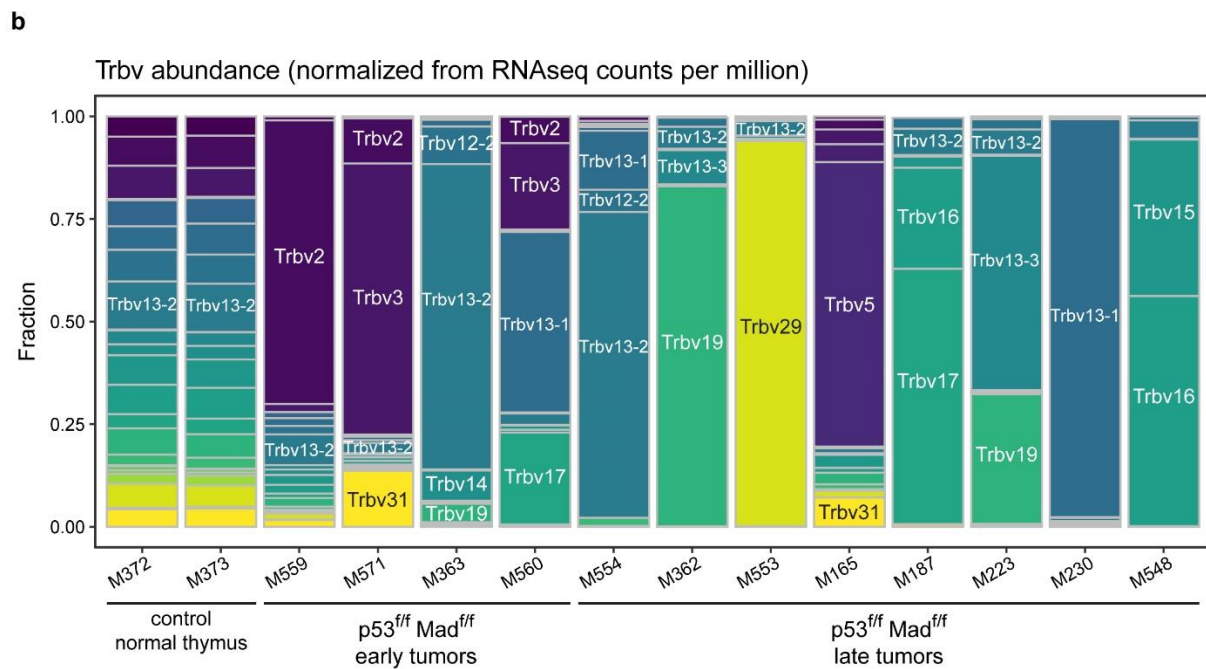
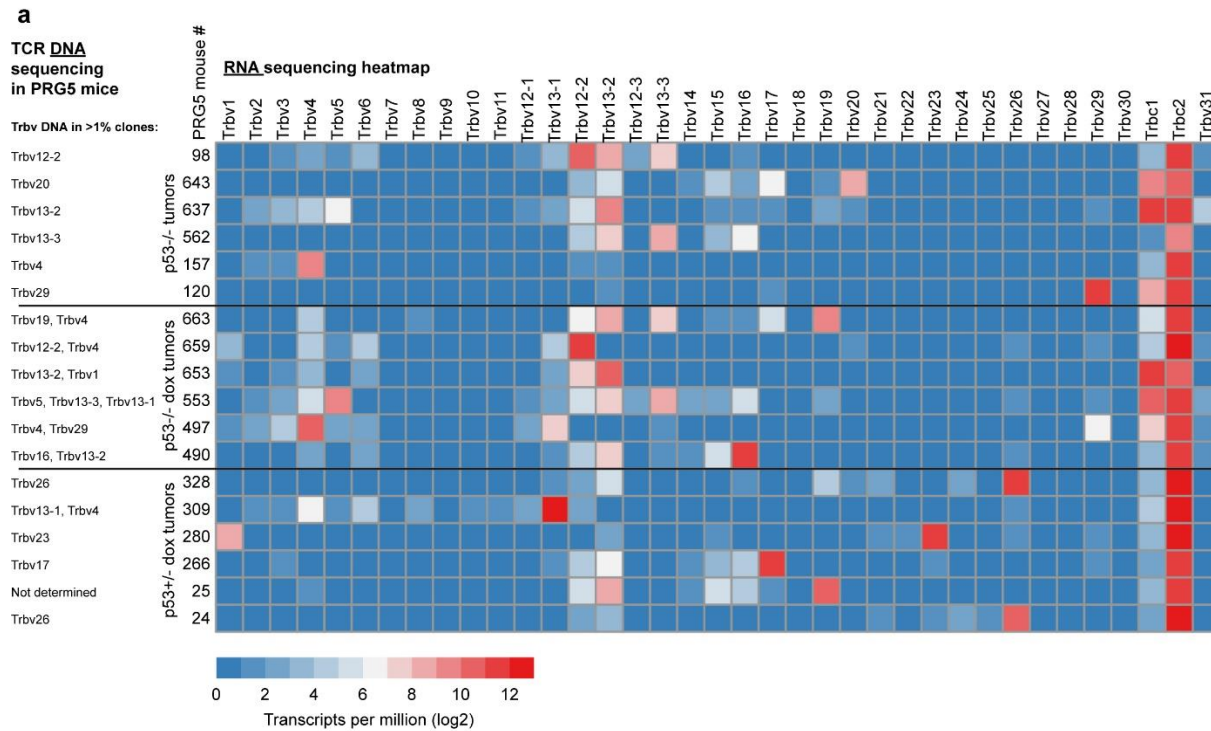


Supplemental Figure S5 | p53 LOH occurs through whole-chromosome mis-segregation without structural changes. (a) Comparison of mRNA expression levels (log[counts per million]) of indicated PRG5 tumors (n=6 tumors from each group) and control thymuses (n=8). Mean \pm SD, and p-values calculated using one-way ANOVA are presented. (b) UCSC genome browser tracks showing RNA expression of exons 2-11 of p53 in indicated mice. (c) CNVkit derived DNA copy number plots of chromosome 11 in tumors from the indicated PRG5 mice. Black line represents the diploid control and the orange line represents the mean copy number of the indicated sample. The location of the *p53* gene is indicated in red. (d) Zoom on exons 2-6 of the p53 gene using Integrated Genome Viewer (IGV 2.3.97) showing number of reads in the indicated samples.

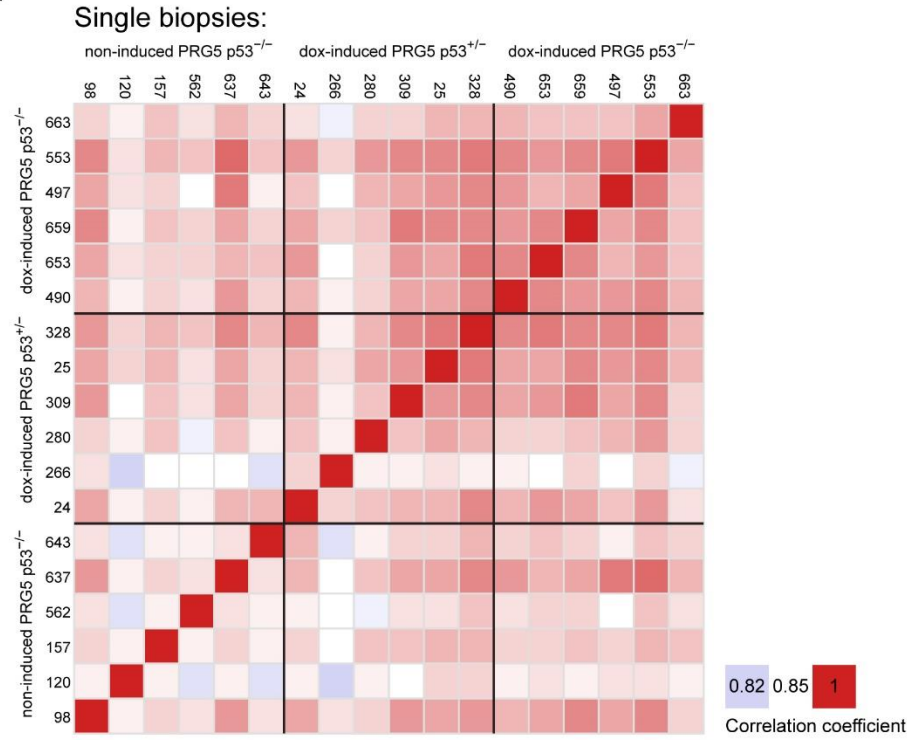
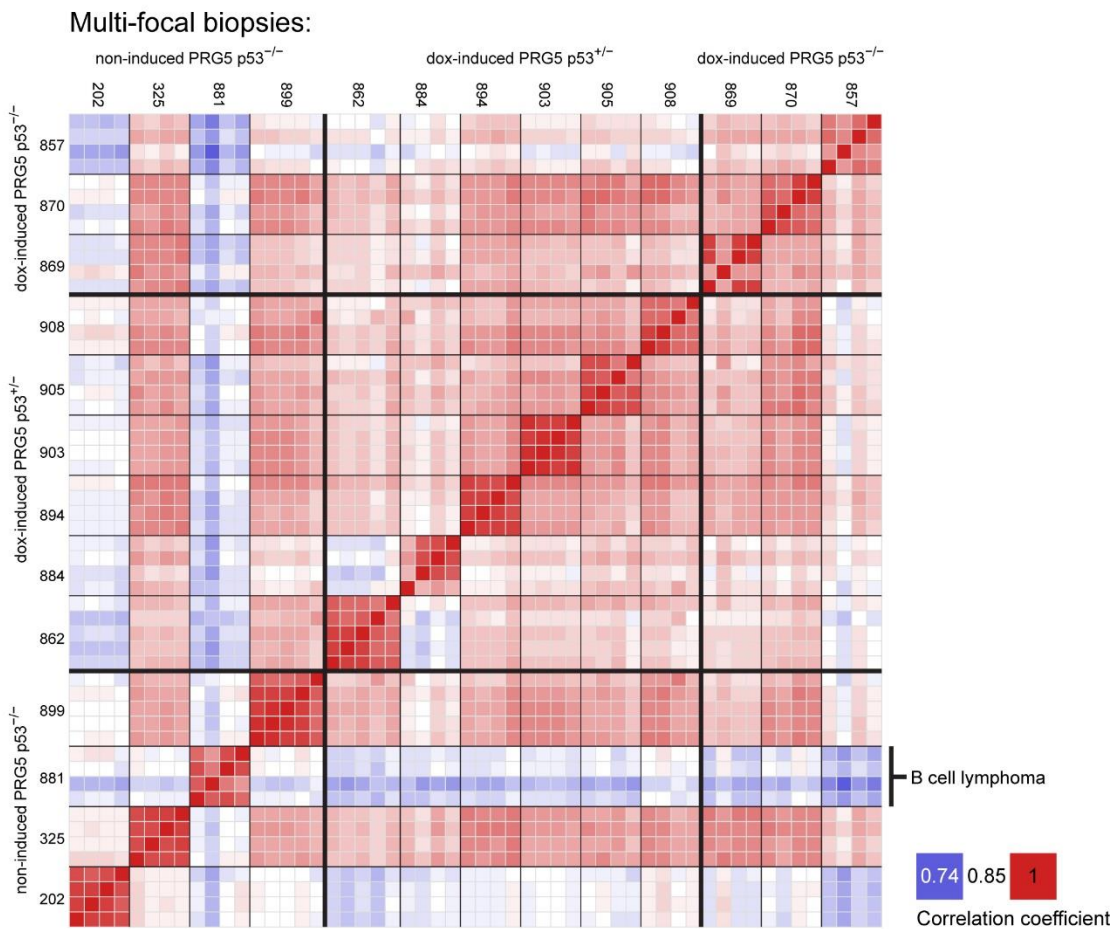


Supplemental Figure S6 | Common molecular events in spontaneous and induced lymphomas. (a) Measurement of centrin-GFP foci in thymic lymphomas from indicated PRG5 mice. Mean \pm SD of $n=6$ ($p53^{-/-}$), $n=5$ ($p53^{-/-}$ 2wk dox), and $n=3$ ($p53^{+/-}$ 2wk dox) are presented. Dashed red line represents the control shown in Figure 2f. (b) Comparison of mRNA expression levels (log[counts per million]) of indicated PRG5 tumors ($n=6$ tumors from each group) and control thymuses ($n=8$). Mean \pm SD, and p -values calculated using one-way ANOVA are presented. (c) Myc protein levels as seen using

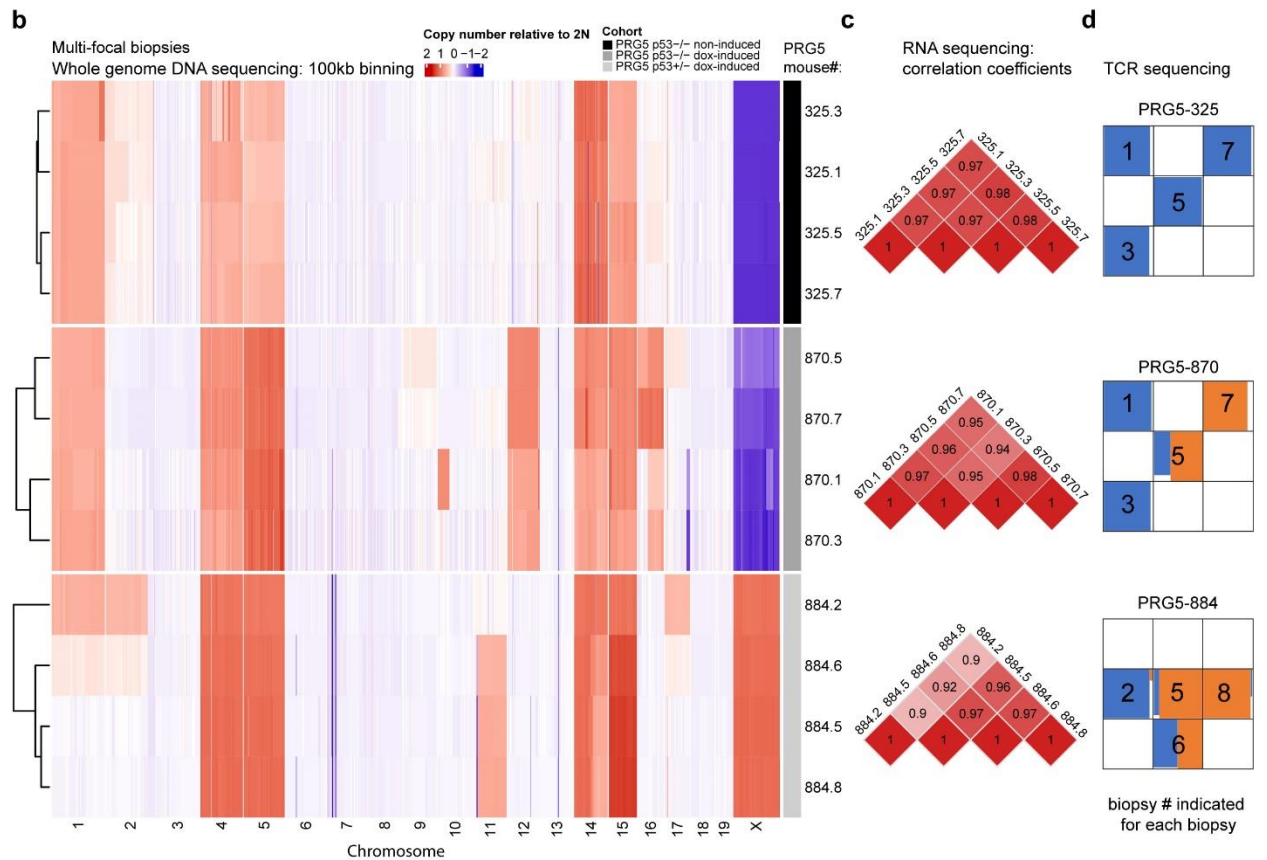
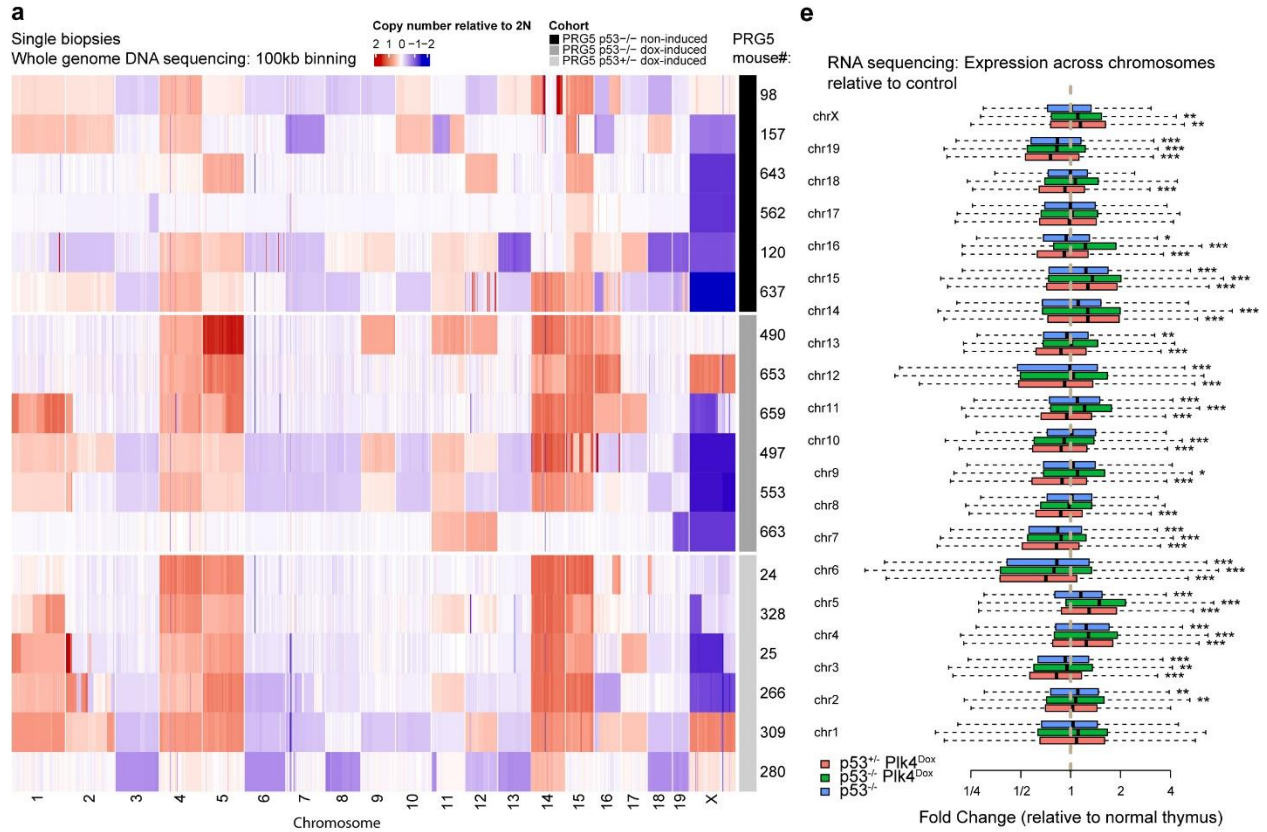
SDS gel electrophoresis immunoblotting in the indicated control or tumor samples. GAPDH is shown as a loading control. **(d)** CNVkit derived DNA copy number plots of chromosome 15 in tumors from the indicated PRG5 mice. Black line represents the diploid control and the orange line represents the mean copy number of the indicated sample. The location of the MYC gene is indicated in red.



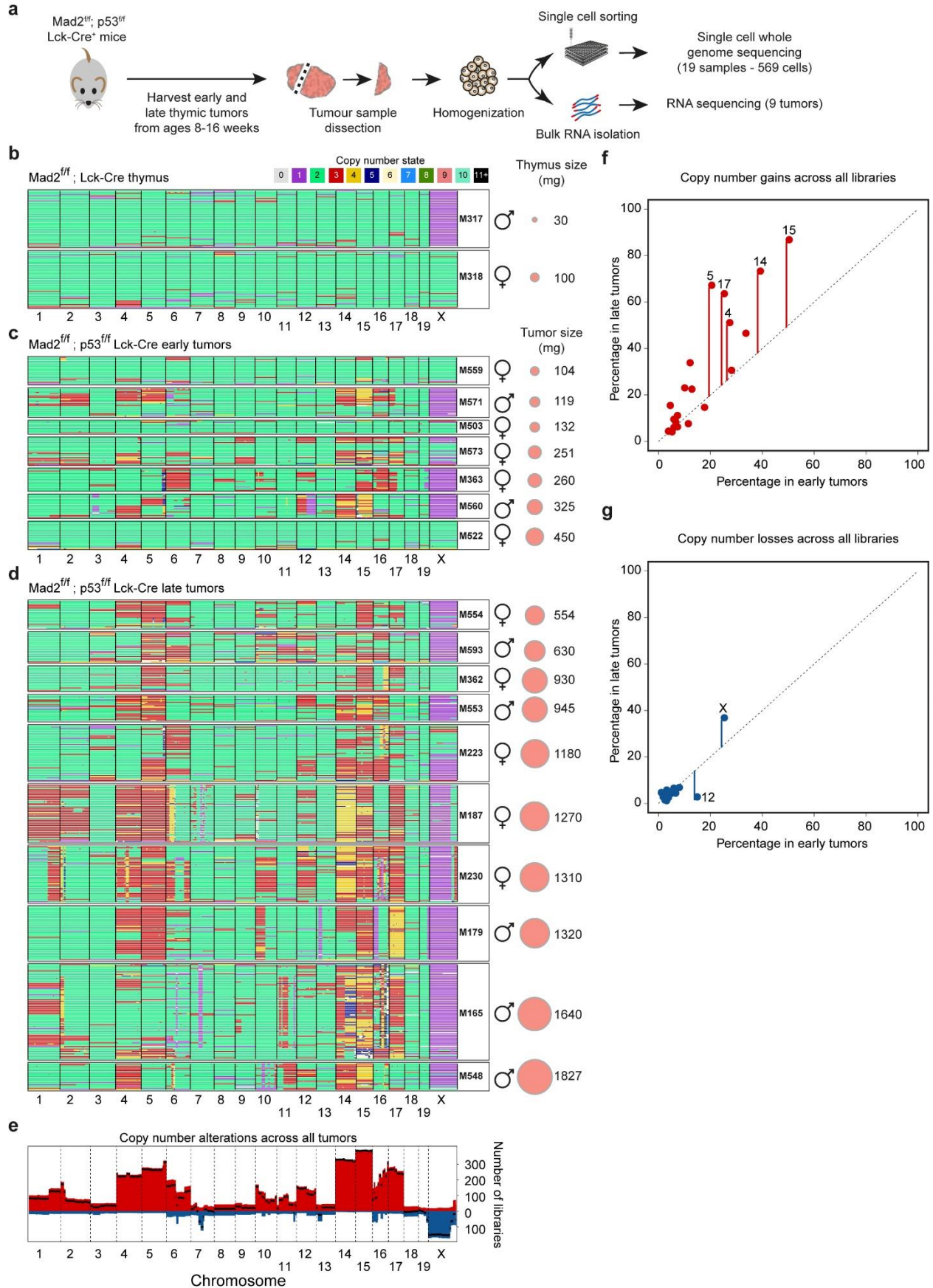
Supplemental Figure S7 | Tumor clonality derived from RNA sequencing data. (a-b) Expression of T cell receptor variable region genes (Trbv genes) as determined using RNA sequencing in tumors from (a) PRG5 mice and (b) Mad2 mice. Trbv genes with frequency > 1% in PRG5 tumors as detected using T cell receptor DNA sequencing (Figure 3a) are shown in a.

a**b**

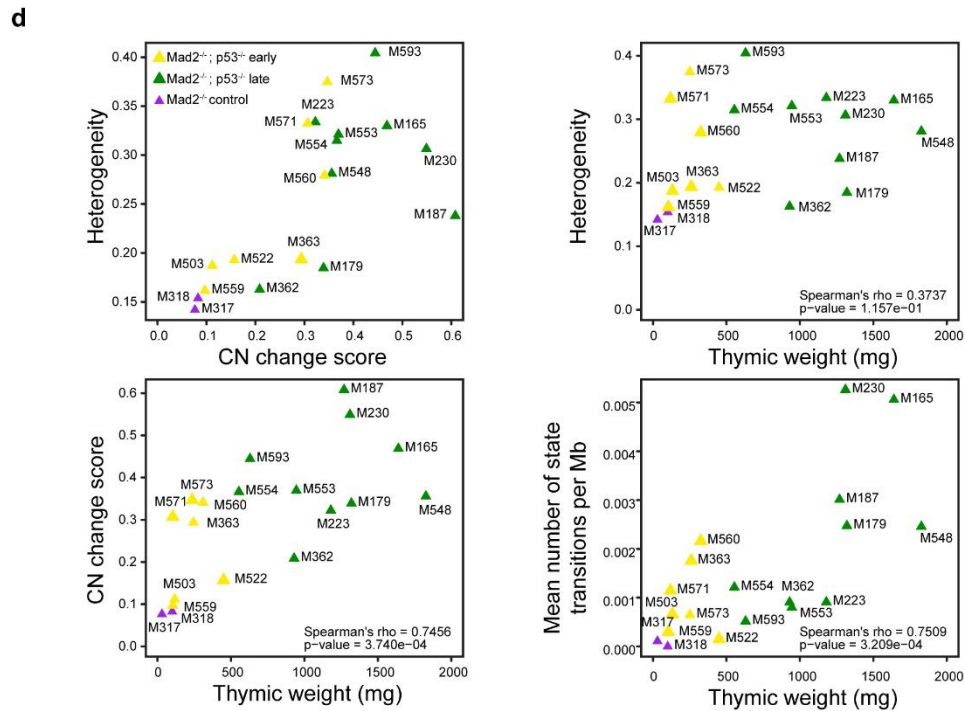
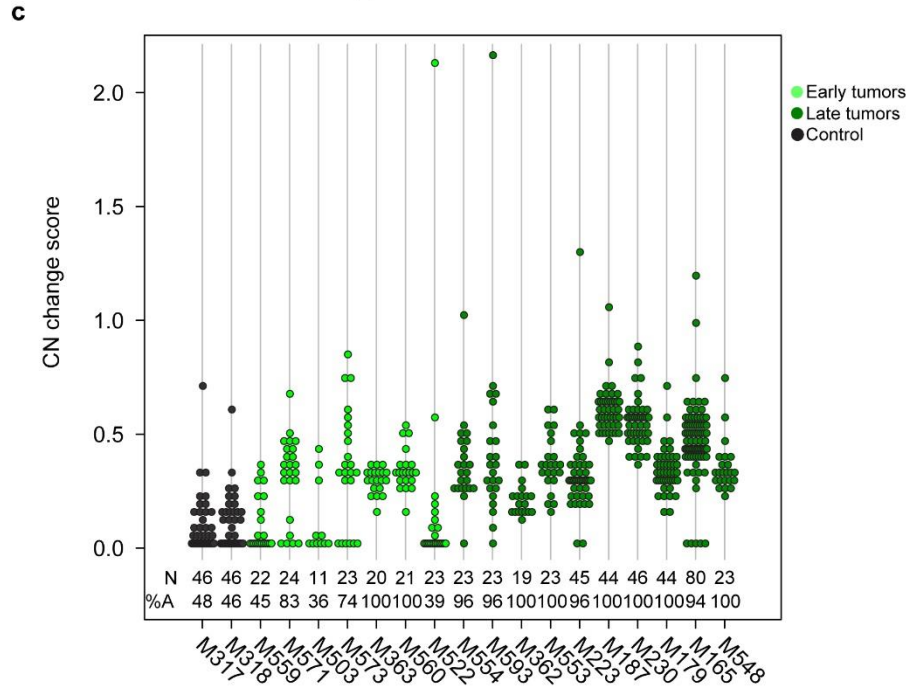
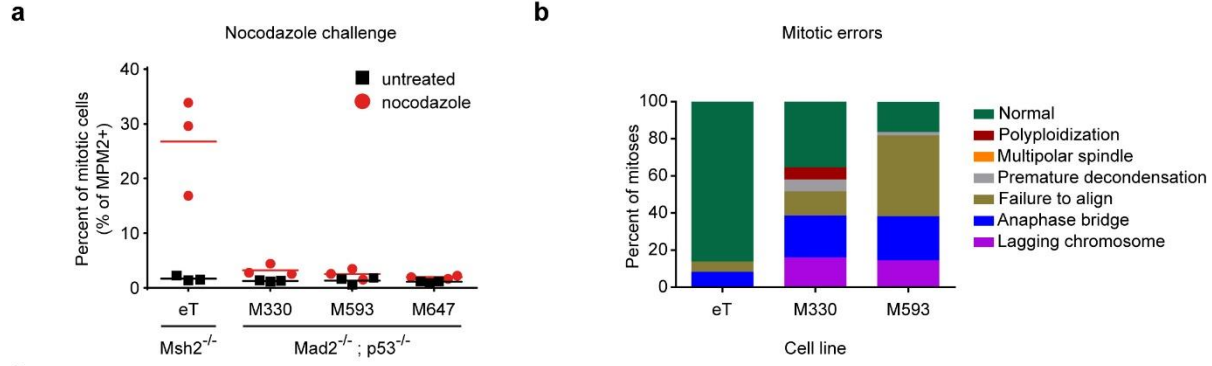
Supplemental Figure S8 | Comparison of CIN-induced and non-induced thymic lymphoma transcriptomes. (a-b) Heatmaps showing pair-wised Pearson correlation coefficients among samples (a - tumor single biopsies, b – multi-focal tumor biopsies) using transcript-per-million (TPM) values as determined using RNA sequencing of the PRG5 mice.



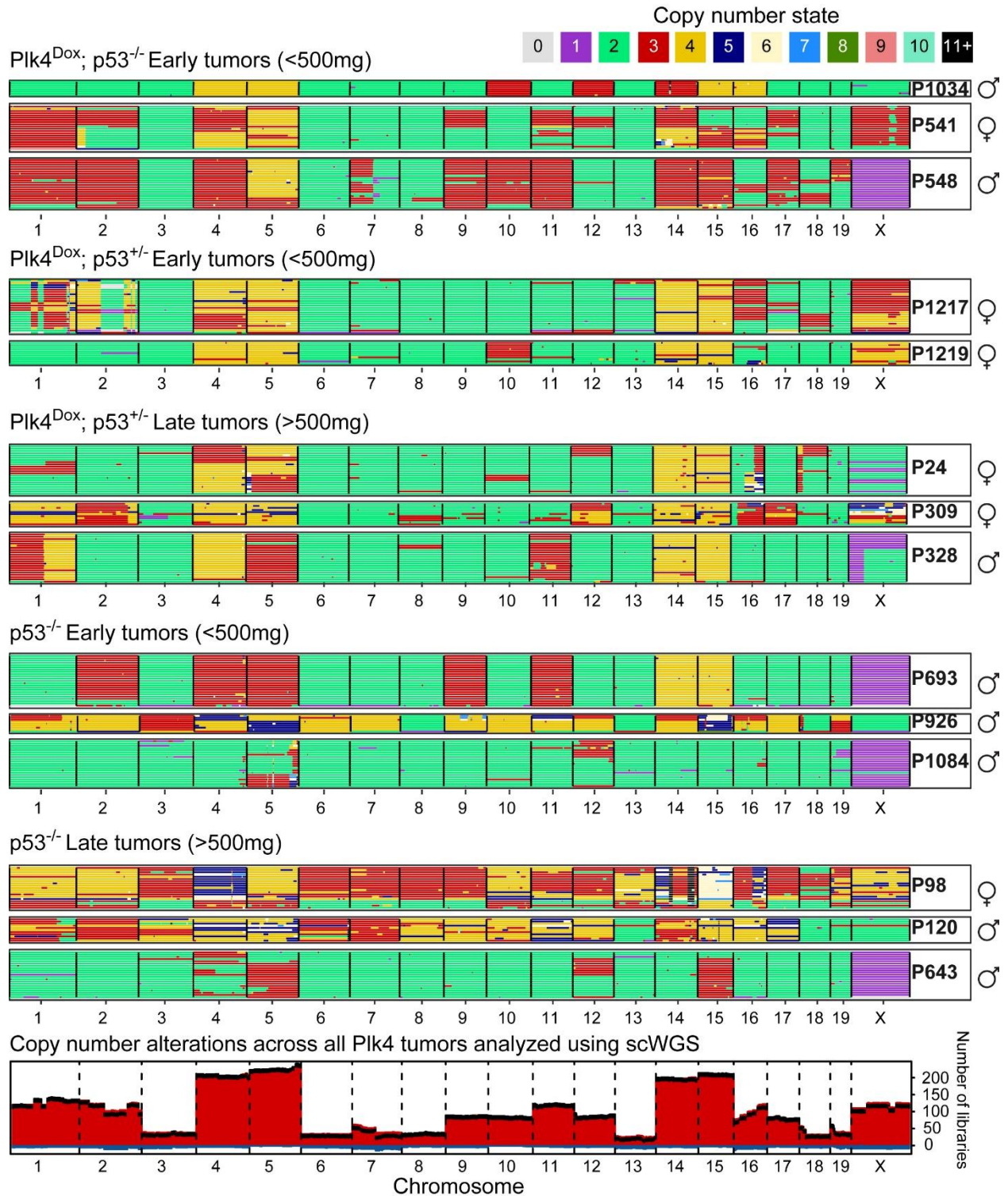
Supplemental Figure S9 | DNA copy number analysis in CIN-induced and non-induced thymic lymphomas. (a) Heatmap showing 100-kb DNA copy number changes in late tumors (>500mg) from non-induced p53^{-/-} PRG5 mice (black), two-weeks doxycycline treated (at the age of 30 days) p53^{-/-} PRG5 mice (dark grey) and p53^{+/-} PRG5 mice (light grey) as determined using whole-genome sequencing. (b) Heatmap showing 100-kb DNA copy number changes in multiple regions taken from late tumors (>500mg) from non-induced p53^{-/-} PRG5 mice (black), two-weeks doxycycline treated (at the age of 30 days) p53^{-/-} PRG5 mice (dark grey) and p53^{+/-} PRG5 mice (light grey) as determined using whole-genome sequencing. (c) Heatmaps showing pair-wised Pearson correlation coefficients among samples using TPM values as determined by RNA sequencing of the indicated PRG5 tumor biopsies. (d) Top ten T cell receptor frequencies (indicative of T cell clones) in thymic T cell lymphomas from PRG5 mice in multi-regional biopsies as determined using T cell receptor sequencing (these samples are also shown in Figure 3b and presented here for convenience). (e) Gene expression levels from each chromosome. The fold change of each gene between each tumor group and the control (n=6 for each group) was calculated, and boxplots of grouping all genes by chromosome for each comparison are presented. p-values (comparing expression levels from individual chromosomes between of each tumor group and the control) were determined using wilcoxon rank sum test, *: p<0.05; **:p<0.01 and ***:p<0.001.



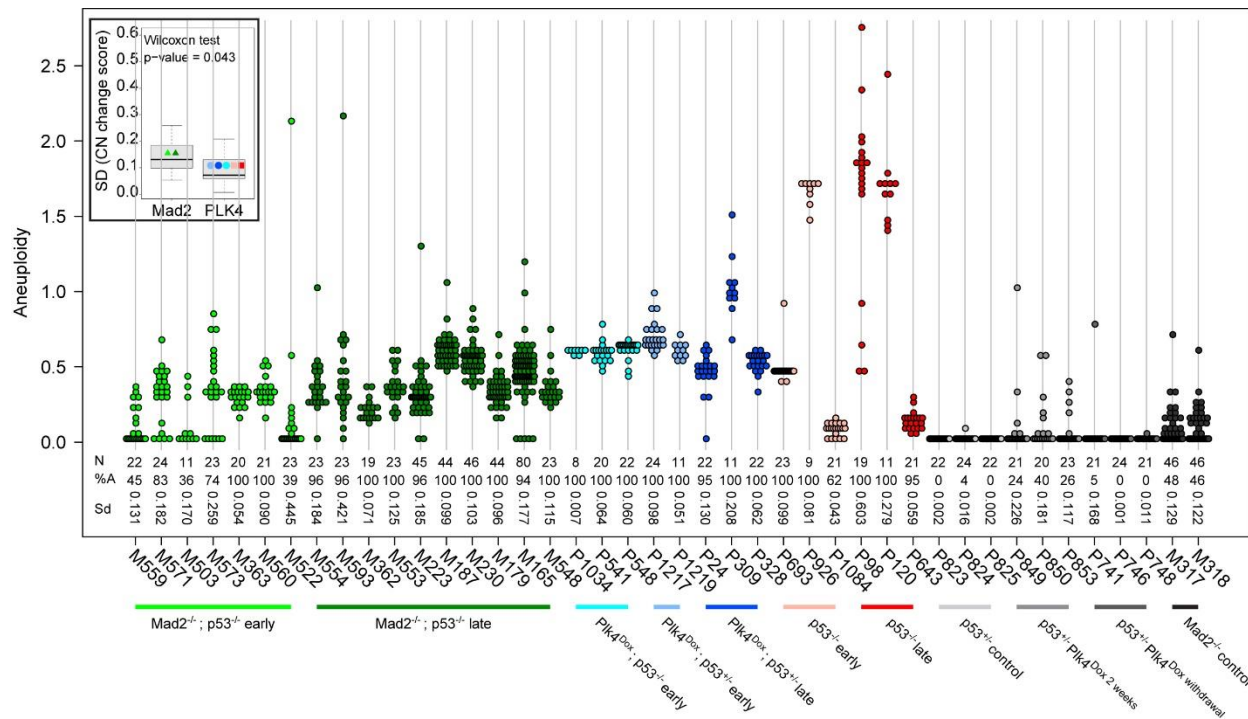
Supplemental Figure S10 | Aneuploidy evolution in thymic lymphomas under chronic CIN driven by deletion of Mad2. (a) Overview of thymic tumors collection from Lck-Cre+; Mad2f/f; p53f/f mice sampled at 8-16 weeks of age. (b-d) Heatmaps showing DNA copy number using single cell whole-genome sequencing of cells collected from (b) Lck-Cre+; Mad2f/f mice (c) Lck-Cre+; Mad2f/f; p53f/f mice with developing (early) tumors and (d) Lck-Cre+; Mad2f/f; p53f/f mice with terminal (late) tumors. Genomic position in order from chromosome 1 to X are in the x-axis and individual cells are in the y-axis. Colors indicate the copy number state as determined by AneuFinder. Data of samples M187 and M179 was previously reported in Foijer et al. *elife*, 2017. Sample M165 is a new sequencing experiment of a sample also shown in Foijer et al. *elife*, 2017. (e) Genome-wide overview of cumulative copy number (1 Mb bins) gains (red) and losses (blue) across all thymic lymphomas presented in panels c-d. Black line presents the net change; difference between number of libraries with a copy number gain and the number of libraries with a copy number loss. (f-g) Comparison of copy number gains (f) and losses (g) between early and late tumors. Each dot represents one chromosome.



Supplemental Figure S11 | Mad2/p53-deficient thymic lymphomas lack a functional SAC and display ongoing CIN. (a) Percentage of mitotic (MPM2+) cells in primary Mad2^{-/-}; p53^{-/-} (M330, M593, M647), or Msh2^{-/-} (euploid Thymic, eT) thymic lymphoma cultures with or without a nocodazole challenge for six hours. (b) Frequency of abnormal mitoses observed in Mad2^{-/-}; p53^{-/-}; (M330, M593), or Msh2^{-/-} (eT) primary thymic lymphoma cultures as determined using live-cell time-lapse imaging after transduction with H2B-mCherry. (c) Analysis of copy number changes of the samples of Figure 1b-d. The numbers below the dot plots indicate the total number of cells and the percentage of cells that has at least one whole chromosome gain or loss. Controls (M317 and M318) are cells sequenced from normal (non-tumor) Mad2^{-/-} (p53 wild-type) mice. (d) Genome-wide karyotype measures (heterogeneity score and CN [copy number] change score) for all samples shown in Figure 1b-d. Structural aberration scores (Mean number of state transitions per Mb) were defined by the number of copy number state transitions per Mb plotted against the weight of the thymus at time of harvest. Correlations were determined using Spearman's rank-order test. See methods for details about the karyotype measures displayed.



Supplemental Figure S12 | Single cell DNA sequencing of early and late PRG5 tumors. (a) Heatmaps showing DNA copy number using single cell whole-genome sequencing of Plk4 induced or control early and late PRG5 tumors with the indicated p53 backgrounds. Genomic position in order from chromosome 1 to X are in the x-axis and individual cells are in the y-axis. Colors indicate the copy number state as determined by AneuFinder. (b) Genome-wide overview of cumulative copy number (1 Mb bins) gains (red) and losses (blue) across all thymic lymphomas presented in panel a. Black line presents the net change; difference between number of libraries with a copy number gain and the number of libraries with a copy number loss.



Supplemental Figure S13 | Differences between chronic and transient CIN in driving thymic lymphomas. Analysis of copy number changes of the entire Mad2 and PRG5 cohorts. The numbers below the dot plots indicate the total number of cells (N), the percentage of cells that has at least one whole chromosome gain or loss (%A) and the standard deviation of the copy number change scores of each sample (Sd). The insert boxplot shows the distribution of standard deviation values of the Mad2 and PLK4 samples. A Wilcoxon rank-sum test was used to determine if there is a significant difference between the SD values of the Mad2 and PLK4 samples.

ID	qvalue
REACTOME_M_PHASE	0.00003
REACTOME_MITOTIC_G1_G1_S_PHASES	0.00003
REACTOME_DNA_REPLICATION	0.00003
REACTOME_S_PHASE	0.00007
KEGG_CELL_CYCLE	0.00011
REACTOME_REGULATION_OF_CHOLESTEROL_BIOSYNTHESIS_BY_SREBP_SREBF	0.00034
REACTOME_CELL_CYCLE_CHECKPOINTS	0.00053
REACTOME_ACTIVATION_OF_ATR_IN_RESPONSE_TO_REPLICATION_STRESS	0.00241
REACTOME_ACTIVATION_OF_GENE_EXPRESSION_BY_SREBF_SREBP	0.00451
REACTOME_DNA_REPLICATION_PRE_INITIATION	0.00481
REACTOME_MITOTIC_PROMETAPHASE	0.00543
REACTOME_SWITCHING_OF_ORIGINS_TO_A_POST_REPLICATIVE_STATE	0.00655
REACTOME_ACTIVATION_OF_THE_PRE_REPLICATIVE_COMPLEX	0.00850
REACTOME_ONCOGENE_INDUCED_SENESCENCE	0.01062
REACTOME_MITOTIC_METAPHASE_AND_ANAPHASE	0.01988
REACTOME_G1_PHASE	0.03175
REACTOME_METABOLISM_OF_STEROIDS	0.03213

Supplemental Figure S14 | Acquisition of the aneuploidy specific profile reshapes gene expression of cell cycle, replication, and stress networks. Significantly enriched pathways (identified using msigdb and R/Bioconductor package clusterProfiler) in PRG5 and Mad2 derived thymic lymphomas with high similarity to the GISTIC analysis using all tumor cohorts as shown in Figure 4 (see gene list in Supplemental Table 5 and heatmap in Figure 6a).

Supplemental Tables (see attached files):

Supplemental Table 1 | Pathological analysis of tissue sections from PRG5 mice.

Supplemental Table 2 | Differentially expressed genes between thymic tumors and control thymuses as determined using RNA sequencing.

Supplemental Table 3 | Top 10 T cell receptor sequences sequences per sample as determined by T cell receptor sequencing

Supplemental Table 4 | Similarity to the GISTIC profile of PRG5 and Mad2 tumors (score ranges between 0-lowest and 1-highest).

Supplemental Table 5 | Gene expression analysis in correlation with the similarity index of each tumor in PRG5 mice (values represent Z scores)